Rg1 protects the MPP+-treated MES23.5 cells via attenuating DMT1 up-regulation and cellular iron uptake

Huamin Xu, Hong Jiang, Jun Wang, Junxia Xie*

State Key Disciplines: Physiology (in incubation), Department of Physiology, Medical College of Qingdao University, Qingdao 266071, China

ARTICLE INFO

ABSTRACT

Ginsenoside-Rg1 is one of the pharmacologically active component isolated from ginseng. Our previous study observed the protective effect of Rg1 on iron accumulation in the substantia nigra (SN) in 1-methyl-4-phenyl-1,2,3,6- tetrahydropyridine (MPTP)-treated Parkinson's disease (PD) mice. However, the mechanisms of this neuroprotective effect of Rg1 are unknown. In this study, we elucidated possible mechanisms for this effect using 1-methyl-4-phenylpyridinium (MPP+)-treated MES23.5 cells. Previous study showed MPP+ treatment induced up-regulation of divalent metal transporter 1 without iron responsive element (DMT1-IRE) in MES23.5 cells. In the present study, we observed that pretreatment with Rg1 could inhibit MPP+-induced up-regulation of DMT1-IRE in MES23.5 cells. Up-regulation of DMT1-IRE by MPP+ treatment was associated with ROS production and translocation of nuclear factor-kappaB (NF-κB) to nuclei, both of which were significantly inhibited by Rg1 pretreatment. The role of ROS and NF-κB in the up-regulation of DMT1-IRE was supported by application of an antioxidant NAC and BAY 11–7082, an inhibitor of IκBα phosphorylation. Furthermore, we also showed Rg1 could decrease DMT1-mediated ferrous iron uptake and iron-induced cell damage by inhibiting the up-regulation of DMT1-IRE. These results indicate that Rg1 protected the MPP+-treated MES23.5 cells via attenuating DMT1-IRE up-regulation likely through inhibition of ROS-NF-κB pathway; Attenuation of DMT1-IRE expression decreased the iron influx and iron-induced oxidative stress.

1. Introduction

Parkinson's disease (PD) is a neurodegenerative disease, characterized by a selective degeneration of dopaminergic neurons in the substantia nigra pars compacta (SNpc) and consequently a reduction in the striatal dopamine levels (Oertel and Ellgring, 1995). Recently, a growing body of evidence shows that selective high levels of iron and oxidative stress resulting from increased iron levels in the SNpc play a key role in PD development (Jiang et al., 2007; Youdim et al., 2004; Zecca et al., 2008). Misregulation of some iron transporters might be involved in this process (Burdo et al., 2001; Jiang et al., 2003; Salazar et al., 2008; Wang et al., 2007).

Iron could be transported into mammalian cells via the transferrin (Tf)-Tf receptor (TfR) and non-transferrin-bound iron (NTBI) pathways. The Tf-TfR was observed unchanged in PD (Faucheux et al., 1993; He et al., 1999), indicating the involvement of NTBI pathway in iron accumulation in PD. Divalent metal transporter 1 (DMT1) is one of the iron transporter involved in NTBI pathway (Gunshin et al., 1997), and increased DMT1 expression was found in the SN of PD models (Burdo et al., 2001; Salazar et al., 2008). There are 4 isoforms of DMT1. At the 5′-end of the gene, alternative promoter usage leads to different transcription start sites at either exon 1A or exon 1B. In the 3′-untranslated region of the mRNA, one possesses iron responsive element (IRE) (termed +IRE), the other does not (termed −IRE) (Hubert and Hentze, 2002; Lee et al., 1998).

Due to the suggested involvement of DMT1 and iron accumulation in PD, some compounds that could regulate iron transporters and then alleviate iron accumulation might have pharmaceutical value in the treatment of PD. Ginsenoside-Rg1, the pharmacologically active component isolated from ginseng (Panax ginseng C.A. Meyer, Araliaceae), was shown to possess anti-inflammatory, antioxidant, anti-amnestic and anti-aging effects (Cheng et al., 2005; Leung et al., 2007; Wakabayashi et al., 1998). Our previous study showed Rg1 could substantially attenuate iron accumulation in the

SN in 1-methyl-4-phenyl-1,2,3,6-tetrahydropyridine (MPTP)-treated PD mice (Wang et al., 2009). Since up-regulation of DMT1-IRE was shown to account for the iron accumulation in 1-methyl-4-phenyl-pyridinium (MPP$^+$)-treated MES23.5 dopaminergic cells (Zhang et al., 2009), we hypothesized that Rg1 might attenuate iron accumulation via regulating DMT1-IRE expression. By using MPP$^+$-treated MES23.5 cells as a model in the study, we elucidated the possible mechanisms how Rg1 affected iron levels. Results showed that Rg1 could attenuate MPP$^+$-induced up-regulation of DMT1-IRE probably through inhibiting ROS-nuclear factor-kappaB (NF-κB) pathway, which decreased the iron influx and iron-induced oxidative stress. This study has provided new evidence for Rg1 to be a potential therapeutic target for the treatment of PD.

2. Materials and methods

2.1. Materials

Unless otherwise stated, all chemicals were purchased from Sigma Chemical Co. (St. Louis. Mo, USA). The primary DMT1-IRE antibody was purchased from the ADI (ADI, San Antonio, TX, USA). The primary NF-κB-p65, PCNA antibodies were from Santa Cruz (Santa Cruz Biotechnology Inc, CA, United States). Calcein-AM was from Molecular Probes (Molecular Probes Inc, Carlsbad, CA, USA). Dulbecco's modified Eagle's medium Nutrient Mixture-F12 (DMEM/F12) were from Gibco (Gibco, Grand Island, NY, USA). Rg1 was purchased from Baiqiuen Medical University. N-acetyl-L-cysteine (NAC) and BAY 11–7082 were from sigma. Other chemicals and regents available were from local commercial sources.

2.2. Cell culture

Dopaminergic cell line MES23.5 cells were offered by Dr. Wei-Dong Le (Baylor College of Medicine, TX, USA), which is a dopaminergic cell line hybridized from murine neuroblastoma-glioma N18TG2 cells with rat mesencephalic neurons exhibiting several properties similar to the primary neurons originated in the SN(Crawford et al., 1992). They were cultured in DMEM/F12 containing Sato's components with 5% FBS, 100 units/ml of penicillin and 100 mg/ml of streptomycin at 37 °C, in a humid 5% CO$_2$, 95% air environment. Ginsenoside-Rg1 was dissolved in absolute alcohol as a concentrated stock and further diluted to their final concentration.

MTT assay showed that the viability of MES23.5 cells treated with MPP$^+$ (<5 μmol/L) for 24 h was unchanged compared to that of control. 10–160 μmol/L MPP$^+$ induced a significant reduction of cell viability (Zhang et al., 2009). In this study, we choose 10 μmol/L MPP$^+$, a relatively low dose, to keep most cells alive, which would help to detect subtle gene expression changes.

For experiments, cells were seeded at a density of $1 \times 10^5/cm^2$ in the plastic flasks or on glass coverslips and were allowed to attach for 24 h before treatment. Then MES23.5 cells were pretreated with Rg1 for 24 h, and subsequently coincubated with MPP$^+$ (10 μmol/L) for 24 h. BAY 11–7082 is an irreversible inhibitor of IκBα phosphorylation, which results in the inhibition of the cytokine-induced NF-κB activation (Pierce et al., 1997; Woods et al., 2000). And NAC can act as a direct ROS scavenger of free radicals (Aruoma et al., 1989). In this study, BAY 11–7082 (2.5 μmol/L) or NAC (500 μmol/L) was added 30 min before insult with MPP$^+$ (10 μmol/L) for 24 h to detect the role of ROS and NF-κB in MPP$^+$ induced DMT1 up-regulation.

2.3. Total RNA extraction and semi-quantitative PCR

Total RNA was isolated by using Trizol Reagent from MES23.5 cells according to the manufacturer's instructions. Then 2 μg of total RNA was reverse-transcribed in a 20 μl reaction using reverse-transcription system. Primers were designed using computer software (Primer Premier 5.0). The following primers were employed for DMT1-IRE: forward 5′-TGGCTGTCACGAGTGCTTACA-3′, reverse 5′-CCATGGCCTTG-GACAGCTATT-3′; Rat GAPDH gene was used as the reference: forward 5′-CCCCC AATGTATCCGTTGTG-3′, reverse 5′-GTAGCCCAGGATGC CCTTTAGT-3′, Amplification and detection were performed with the following conditions: an initial hold at 95 °C for 10 s followed by 40 cycles at 95 °C for 5 s and 60 °C for 45 s.

2.4. Preparation of nuclear extract

For immunoblot analysis, the extraction and isolation of nuclear and cytoplasmic protein were performed according to the Nuclear and Cytoplasmic Protein Extraction Kit (Beyotime, Jiangsu, China). After washing with 1 mL ice-cold PBS, the cells were collected and then centrifuged for 5 min at 1200 rpm at 4 °C and the pellet was dissolved with cytoplasmic protein extraction agent A supplemented with PMSF. After 5 s vortex, the tubes were incubated for 10–15 min on ice to promote lysis. Then the cytoplasmic protein extraction agent B was added, vortexed for 5 s and incubated on ice for 5 s. The samples were then centrifuged for 5 min at 14,000 g at 4 °C and the supernatant, containing the cytosolic fraction, was immediately frozen for further analysis. The pellet was resuspended in nuclear protein extraction agent supplemented with PMSF. After 15–20 times vortex for 30 min and 14,000 g centrifuging for 10 min, the supernatants containing the nuclear extracts were obtained.

2.5. Western blots

Cells were lysed directly on the culture dishes using lysis buffer (50 mmol/L Tris·HCl, 150 mmol/L NaCl, 1% Nonidet-40, 0.5% sodium deoxycholate, 1 mmol/L EDTA) plus 1 mmol/L PMSF and protease inhibitors (1 μg/ml pepstatin, 1 μg/ml aprotinin, 1 μg/ml leupeptin). The protein concentration was determined by the Bradford assay kit (Bio-Rad Laboratories, Hercules, CA). Sixty micrograms total proteins were separated using 10% SDS-polyacrylamide gels and then transferred to PVDF membranes. After overnight blocking with 5% non-fat milk at 4 °C, the membranes were incubated with rabbit anti-rat DMT1-IRE antibody (1:2000, ADI, USA) or NF-κB polyclonal antibody (1:200, Santa Cruz) for 2 h at room temperature. β-actin was detected by mouse anti-β-actin monoclonal antibody (1:10000, Sigma, USA) according to similar procedures to ensure equal sample protein loading, and mouse anti-rat PCNA antibody (1:200, Santa Cruz) was used to ensure equal sample protein loading for nuclear extract. Anti-rabbit and anti-mouse secondary antibodies conjugated to horseradish peroxidase were used at a dilution of 1:10000. Cross-reactivity was visualized using ECL western blotting detection reagents and then was analyzed through scanning densitometry by Tanon Image System.

2.6. Reactive oxygen species (ROS) assay

The production of ROS was assessed by the oxidation of 2′, 7′-dichlorodihy-drofluorescein diacetate (H$_2$DCFDA; Sigma) as described before (Chwa et al., 2006; Yang et al., 2007; Yao et al., 2008; Zhang et al., 2009). After washing 3 times with PBS, cells were incubated in DMEM/F12 containing H$_2$DCFDA (10 μmol/L) for 30 min. The fluorescence signals were measured with excitation filter of 488 nm and 525 nm emission wavelengths.

2.7. Calcein loading of cells and ferrous iron influx assay

Ferrous iron influx into MES23.5 cells was determined by the quenching of calcein fluorescence as described before (Wetli et al., 2006; Zhang et al., 2009). Cells were incubated with calcein-AM (0.5 μmol/L final concentration) in HEPES-buffered saline (HBS, 10 mmol/L HEPES, 150 mmol/L NaCl, pH = 7.4) for 30 min at 37 °C. The excess calcein on cell surface was washed out 3 times with HBS. The coverslips were mounted in a perfused heated chamber. Calcein fluorescence was recorded at 488 nm excitation and 525 nm emission wavelengths and fluorescence intensity was measured every 3 min for 30 min while perfusing with 1 mM ferrous iron (ferrous sulfate in ascorbic acid solution, 1:44 molar ratio, pH = 6.0), prepared immediately prior to the experiments (Picard et al., 2000). The mean fluorescence signal of 25–30 single cells in four separate fields was monitored at 200× magnification and processed with Fluoview 5.0 Software.

2.8. Detection of mitochondrial transmembrane potential (ΔΨm)

Changes in the mitochondrial membrane potential were measured by rhodamine123 using flow cytometry (Becton Dickinson, USA) in MES23.5 cells. Cells in different groups were incubated in 100 μmol/L ferrous iron (pH = 6.0) for 3 h, and then incubated with rhodamine123 in a final concentration of 5 μmol/L for 30 min at 37 °C. After washing twice with HBS, fluorescence was recorded at 488 nm excitation and 525 nm emission wavelengths.

2.9. Statistical analysis

Each experiment was performed at least three times, and the results are presented as mean ± S.E.M. One-way analysis of variance (ANOVA) was used to compare the differences between means. Influx studies were carried out by the two ways ANOVA followed by Student-Newman-Keuls test and data were presented as mean ± S.D. A level of $P < 0.05$ was considered to be significant.

3. Results

3.1. Rg1 decreased ROS production in the MPP$^+$-treated MES23.5 cells

It was reported that the protective effect of Rg1 was mostly attributed to its antioxidant effect acting as a free-radicals scavenger (Chen et al., 2003; Lim et al., 1997; Lopez et al., 2007; Zhong and Jiang, 1997). Therefore, we observed the effect of different concentration of Rg1 on MPP$^+$-induced ROS production in MES23.5 cells to confirm whether Rg1 had protective effect on MPP$^+$ in

MES23.5 cells and choose an optimal concentration of Rg1 to test its biological effects in MPP$^+$-treated cells.

As shown in Fig. 1, there was a significant 37.6% increase in the levels of ROS in MPP$^+$-treated cells compared with that of control. However, cells pretreated with 10^{-5} mol/L, 10^{-6} mol/L, 10^{-7} mol/L and 10^{-8} mol/L Rg1 could cause a 31.8%, 36.0%, 31.8%, 26.3% decrease in ROS production, respectively, compared to that of the MPP$^+$ treatment (Fig. 1). Therefore, 10^{-6} mol/L Rg1 which showed highest effect on reduction of ROS production was chosen for the following experiments.

No significant changes were observed in cell viability with individual 10^{-5}–10^{-8} mol/L Rg1 for 48 h (Data not shown), indicating that Rg1 had little cytotoxic effect on MES23.5 cells at the concentration range.

3.2. Rg1 attenuated up-regulation of DMT1-IRE in MPP$^+$-treated MES23.5 cells

Our previous study showed DMT1-IRE was up-regulated in MPP$^+$-treated MES23.5 dopaminergic cells and this up-regulation accounted for the iron accumulation in these cells (Zhang et al., 2009). Thus we hypothesized that Rg1 might attenuate iron accumulation in MPP$^+$-treated MES23.5 cells via regulating iron transporter DMT1-IRE gene expression.

To confirm this hypothesis, we detected the protein and mRNA levels of DMT1-IRE in MES23.5 cells with different treatments. As shown in Fig. 2(2A and 2B), DMT1-IRE protein in MPP$^+$-treated MES23.5 cells was up-regulated to 54% compared to the control, while Rg1 could prevent this up-regulation of DMT1-IRE protein. To further investigate whether this reduced expression of DMT1-IRE protein was due to the decreased DMT1 mRNA transcription, semi-quantitative PCR was conducted to measure DMT1 mRNA levels. There was a 68% increase of DMT1-IRE mRNA in MPP$^+$-treated cells compared with that of the control. And Rg1 pretreatment reversed this MPP$^+$-induced increase of DMT1-IRE mRNA (Fig. 2C and D). This indicated Rg1 could attenuate the increase expression of DMT1-IRE at both mRNA and protein levels caused by MPP$^+$.

3.3. Rg1 prevented the MPP$^+$-induced translocation of NF-κB to nucleus

NF-κB acting on NF-κB binding sites on the DMT1 promoter might play a role in the expression of this transporter (Huang et al., 2006).

Then we hypothesized that Rg1 might regulate the expression of DMT1-IRE through inhibiting NF-κB activation in MPP$^+$-treated cells. To further confirm our hypothesis, we detected the expression of NF-κB-p65 in the cytoplasm and nucleus, respectively. As shown in Fig. 3, 10 μmol/L MPP$^+$ could reduce the protein levels of NF-κB-p65 in the cytoplasma and increase its levels in nucleus, suggesting that MPP$^+$ could activate NF-κB translocation from cytoplasm to nucleus. However, when pretreated with Rg1, this MPP$^+$-induced decreases of NF-κB-p65 expression in cytoplasma and increases in nucleus were significantly inhibited, indicating the increased translocation of NF-κB was inhibited by Rg1 (Fig. 3).

3.4. NF-κB and ROS were involved in the MPP$^+$-induced up-regulation of DMT1-IRE

To further confirm the role of NF-κB in the up-regulation of DMT1-IRE in MPP$^+$-treated cells, BAY 11-7082 (an irreversible inhibitor of IκBα phosphorylation which results in the inhibition of the cytokine-induced NF-κB activation) was chosen in this study. As shown in Fig. 4, DMT1-IRE protein levels in MPP$^+$-treated MES23.5 cells were significantly up-regulated compared to the control. Pretreated with 2.5 μM BAY 11–7082 could reverse the MPP$^+$-induced up-regulation of DMT1-IRE in MES23.5 cells, indicating the involvement of NF-κB activation in this process (Fig. 4).

Evidence proved that oxidative stress-induced ROS generation has been implicated in NF-κB activation (Pyo et al., 2008). Therefore, we hypothesized that Rg1 might have the regulatory effect on NF-κB and DMT1-IRE by its antioxidant effect. Thus a direct ROS scavenger of free-radicals NAC was used in this study. Results showed 0.5 mmol/L NAC could also prevent the up-regulation of DMT1-IRE. This suggested ROS was also involved in this process.

3.5. Rg1 attenuated DMT1-mediated ferrous iron influx in MPP$^+$-treated MES23.5 cells

Up-regulation of DMT1-IRE could enhance iron uptake and increase the intracellular ferrous iron levels. To find out whether Rg1 has neuroprotective effect on DMT1-mediated iron uptake in MES23.5 cells, fluorescence dye calcein was used to measure the ferrous iron influx of MES23.5 cells after perfusing with 1 mmol/L ferrous iron. The fluorescence intensity decreased, indicating the extracellular ferrous iron was transported into cells. Results showed that there was more rapid fluorescence quenching and
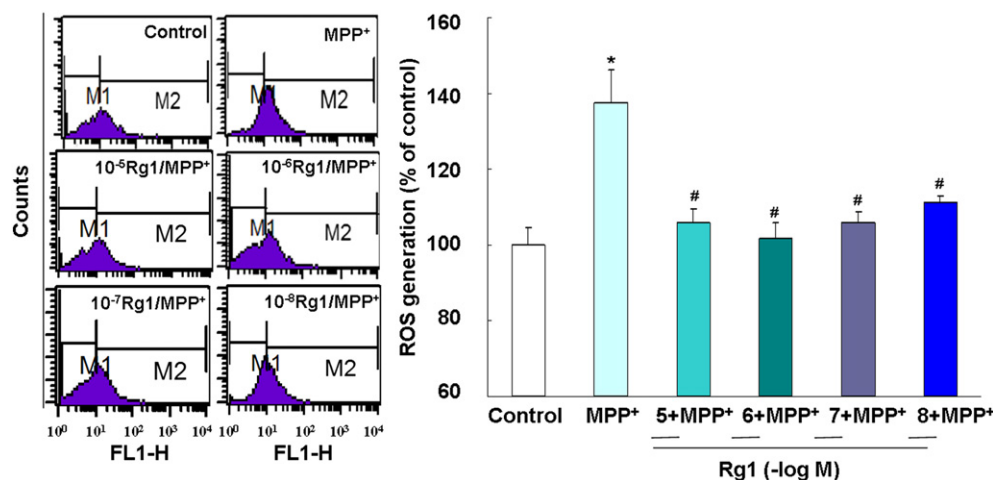
Fig. 1. Rg1 decreased the ROS production of MPP$^+$ treated MES23.5 cells. 10 μmol/L MPP$^+$ increased the production of ROS in MES23.5 cells compared to the control, while cells pretreated with Rg1(10^{-5}–10^{-8} mol/L) showed a decreased levels of ROS compared to MPP$^+$. Fluorescence values of the control were set to 100%. Data were presented as mean ± S.E.M. of 6 independent experiments. $^*P < 0.05$, compared to the control. $^\#P < 0.05$, compared to MPP$^+$ treated cells.
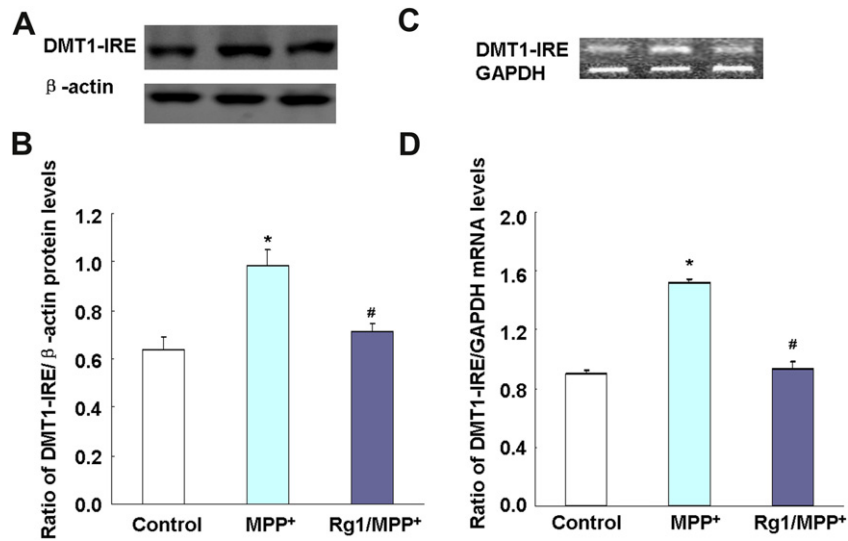
Fig. 2. Rg1 attenuated DMT1 up-regulation in the MPP^+-treated MES23.5 cells. A: Increased expression of DMT1-IRE protein was observed in MPP^+-treated cells. When pretreated with Rg1 (10^{-6} mol/L), the protein levels of DMT1-IRE decreased compared with MPP^+-treated cells. β-actin was used as a loading control. B: Bar graphs for protein levels of DMT1-IRE. C: mRNA levels of DMT1-IRE were increased in MPP^+-treated MES23.5 cells compared to the control. When pretreated with Rg1, the mRNA levels decreased significantly compared to MPP^+ group. D: Bar graphs for mRNA levels of DMT1-IRE. Data were presented as mean ± S.E.M. of 6 independent experiments. [*]$P < 0.01$, compared to the control; [#]$P < 0.01$, compared to MPP^+ group.

a significant decrease in the fluorescence intensity in MPP^+-treated cells compared with the control when perfusing with 1 mmol/L ferrous iron. The fluorescence intensity restored to the control levels when pretreated with Rg1 (Fig. 5). This indicated that Rg1 could suppress the increased ferrous iron influx mediated by increased expression of DMT1.

3.6. Rg1 prevented increased iron-induced cell damage in MES23.5 cells

MPP^+-induced up-regulation of DMT1-IRE could increase ferrous iron influx into cells. Excess ferrous iron could react with hydrogen peroxide and produce highly ROS; this aggravated the intracellular
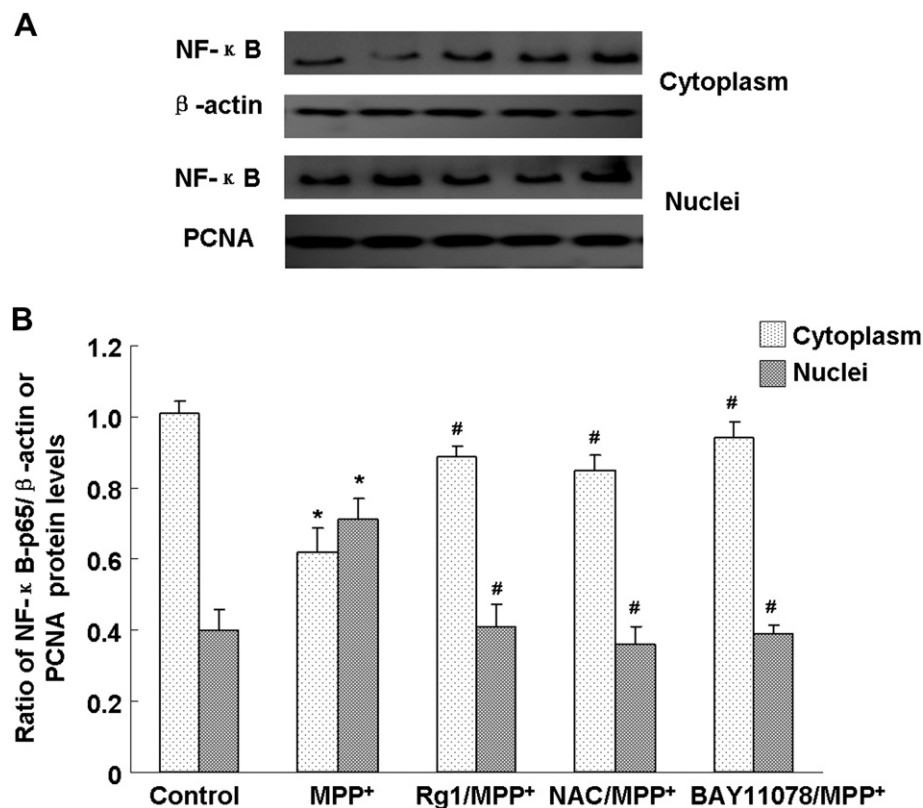

Fig. 3. Rg1 prevented the MPP^+-induced translocation of NF-κB to nucleus. A: The expression of NF-κB-p65 in cytoplasm and nucleus were both detected by western blots. Data showed 10 μmol/L MPP^+ could activate translocation of NF-κB from cytoplasm to nucleus, while when pretreated with Rg1, the translocation of NF-κB was inhibited. B: Bar graphs. Data were presented as mean ± S.E.M. of 6 independent experiments. [*]$P < 0.01$, compared to the control; [#]$P < 0.01$, compared to MPP^+ group.
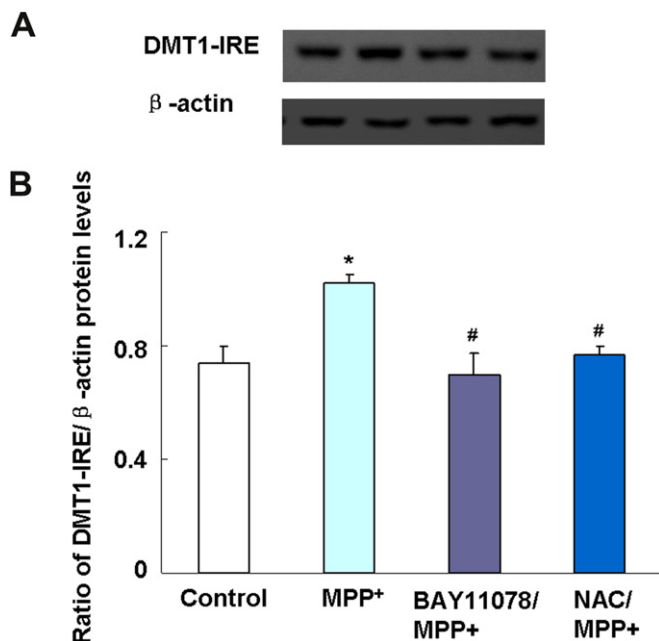
Fig. 4. BAY 11–7082 and NAC inhibited MPP$^+$-induced up-regulation of DMT1-IRE in MES23.5 cells. A. Western blots were applied to detect the protein levels of DMT1-IRE. Results showed BAY 11–7082 and NAC could abolish the MPP$^+$-induced up-regulation of DMT1-IRE in MES23.5 cells. B: Bar graphs. Data were presented as mean $\pm$ S.E.M. of 6 independent experiments. $^*P < 0.01$, compared to the control. $^\#P < 0.05$, compared to MPP$^+$ group. $^\wedge P < 0.01$, compared to the control; $^\$P < 0.01$, compared to MPP$^+$ group.

ROS levels and induced the dysfunction of mitochondrion. To further investigate if Rg1 could inhibit this damage, we measured ROS production and the mitochondrial membrane potential changes in MPP$^+$-treated cells followed by iron incubation. The intracellular ROS levels were detected using a fluorescence sensitive probe (H$_2$DCF-DA). As shown in Fig. 6A and C, when MPP$^+$-treated cells incubated with 100 μmol/L ferrous iron, they showed a significant
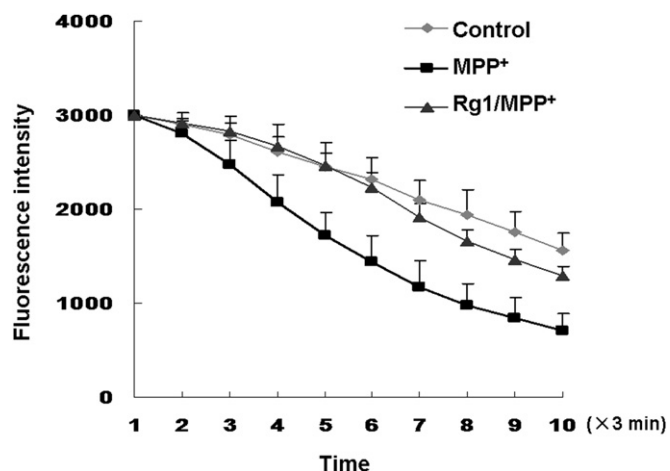
Fig. 5. Ferrous iron influx into MES23.5 cells in different groups. Ferrous iron influx function was detected by confocal using calcein fluorescence. The fluorescence intensity represented the mean value of 35 separate cells from four separate fields at each time point and was presented as mean $\pm$ S.D. of 6 independent experiments. When perfusing different groups of MES23.5 cells with 1 mmol/L ferrous iron, fluorescence intensity in MPP$^+$ treated cells decreased more rapidly compared to the control. And there was a significant increase of fluorescence intensity in Rg1 pretreated cells compared with solely MPP$^+$ treated cells. (Two-way ANOVA, $F = 29.265$, $P < 0.01$, cells treated with MPP$^+$ compared to the control; $P < 0.01$, cells pretreated with Rg1 compared to cells treated with MPP$^+$).

58% increase in the levels of ROS compared to the solely iron treatment. This could be suppressed by Rg1 pretreatment. Then changes in the mitochondrial membrane potential were measured by rhodamine123. As shown in Fig. 6B and 6D, there was a significant 27% decrease of $\Delta\Psi$m in MPP$^+$-treated cells when incubated with ferrous iron compared to the control. Cells solely incubated in ferrous iron only showed 16% reduction. Pretreatment with Rg1 for 24 h could inhibit this reduction.

4. Discussion

This study showed the neuroprotective effects of Rg1 on MPP$^+$-treated dopaminergic MES23.5 cells and revealed the underlying mechanisms. Our results suggested that Rg1 could attenuate MPP$^+$-induced up-regulation of DMT1-IRE through inhibition of ROS-NF-κB pathway, resulting in the decreased ferrous iron influx and cell survival.

MPP$^+$ is a common neurotoxin used as an agent for inducing PD models. It could enter the cell through the dopamine reuptake system, and then inhibit complex I of the mitochondrial respiratory chain, and may induce oxidative stress (Cassarino et al., 1999; Desai et al., 1996). It was reported that the protective effect of Rg1 was mostly attributed to its antioxidant effect acting as a free-radicals scavenger (Chen et al., 2003; Lim et al., 1997; Lopez et al., 2007; Zhong and Jiang, 1997). Therefore, ROS production was first detected to confirm whether Rg1 had protective effect on MPP$^+$-treated MES23.5 cells. Results demonstrated that Rg1 significantly decreased the MPP$^+$-induced ROS production. This is also consistent with other previous work that Rg1 could suppress oxidative stress in MPTP-treated PD mice (Chen et al., 2005).

Iron is essential for vital cellular activities and also found throughout the brain for its important role including brain oxygen transport, electron transfer, neurotransmitter synthesis and myelin production. However, due to its highly reactive nature, excess iron could lead to the generation of oxidative stress, which is toxic to cells. Elevated iron levels in the SNpc have been found in PD. However, the underlying mechanisms of iron accumulation in this region are largely unknown. Previous studies showed that DMT1-dependent increase in iron levels played a key role in the death of dopaminergic neurons in PD. G185R mutation that impairs DMT1 iron transport decreases the susceptibility of microcytic mice (mk/mk) and Belgrade rats to MPTP-induced and 6-hydroxydopamine (6-OHDA)-induced neurotoxicity, respectively (Salazar et al., 2008). This convinced the important role of DMT1 and DMT1-dependent iron transport in MPTP or 6-OHDA-induced neurotoxicity. Therefore, DMT1 might be a new pharmacological target to treat PD. Some compounds that could attenuate the expression of DMT1 in the SNpc might have some pharmaceutical value in the treatment of PD.

Our previous study showed Rg1 could substantially attenuate iron accumulation in the SN in MPTP-treated PD mice (Wang et al., 2009). And up-regulation of DMT1-IRE was shown to account for iron accumulation in MPP$^+$-treated MES23.5 dopaminergic cells (Zhang et al., 2009). In this study, we investigated whether Rg1 had the protective effect on MPP$^+$-induced up-regulation of DMT1-IRE. Results showed Rg1 pretreatment could prevent the MPP$^+$-induced up-regulation of DMT1-IRE, suggesting Rg1 could affect the intracellular iron levels by regulating the expression of DMT1-IRE.

However, the mechanisms underlying the regulation of Rg1 on DMT1-IRE were not understood. The regulating of DMT1+IRE was proved to be dependent on IRE/IRP (iron regulatory protein) system (Lee et al., 1998). However, the regulation of gene expression of DMT1-IRE was not fully elucidated. It is postulated that transcription factors acting on NF-κB binding sites on the DMT1 promoter may play a role in the expression of the transporter (Huang et al., 2006). NF-κB is constitutively expressed as a cytoplasm p50/p65
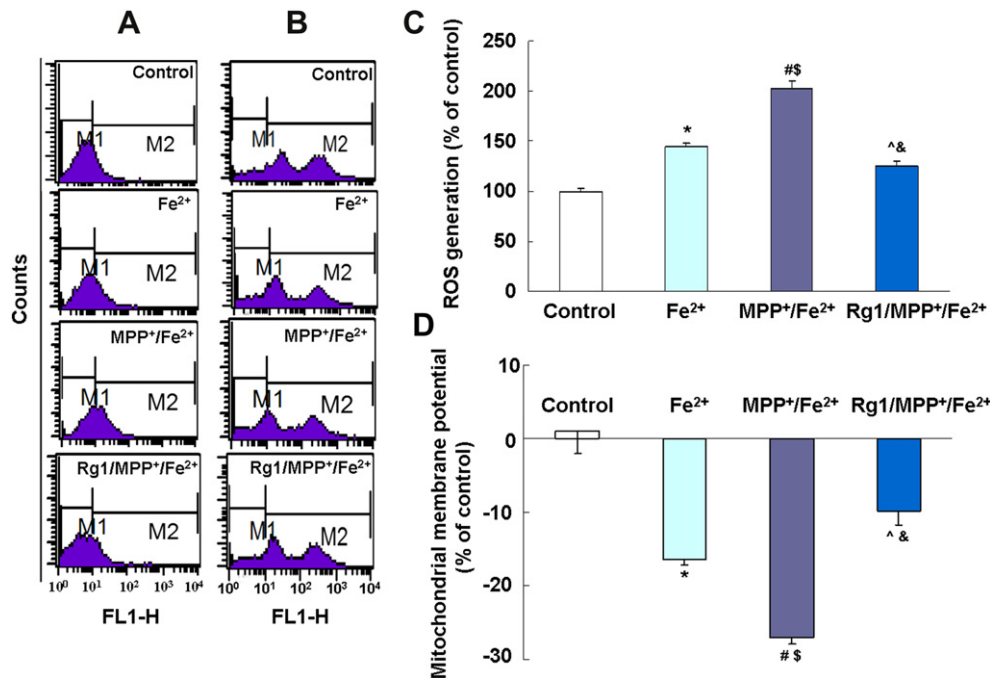
Fig. 6. Rg1 prevented increased iron-induced cell damage including ROS production (A, C) and $\Delta\Psi m$ (B, D) in MES23.5 cells followed by iron incubation. A: Representatives of the fluorometric assay on ROS. There was a significant increase in the levels of ROS when incubated with ferrous iron in MPP$^+$-treated cells. This increase of ROS could be suppressed by Rg1 pretreatment. B: Representatives of the fluorometric assay on $\Delta\Psi m$ of different groups. When MPP$^+$-treated cells incubated in 100 μmol/L ferrous iron, they showed a significant decrease of $\Delta\Psi m$. Pretreatment with Rg1 for 24 h could attenuate this reduction. Statistical analysis was presented as C and D. Data were presented as mean $\pm$ S.E.M. of 6 independent experiments. Fluorescence values of the control were set to 100%. $^*P < 0.01$, $^\#P < 0.01$, compared to control; $^\$P < 0.01$, $^\&P < 0.05$, compared to Fe^{2+}; $^\wedge P < 0.01$, compared to MPP$^+$/Fe^{2+}.

heterodimer bound to an inhibitory subunit, IκB (Lenardo and Baltimore, 1989). Exposure of cells to various pathological stimuli activated NF-κB and promoted the translocation of NF-κB from cytoplasm to nucleus, and then regulated the target gene expression (Pahl and Baeuerle, 1997). Paradkar et al. found NF-κB nuclear translocation and the subsequent binding to the putative NF-κB response element (at -19 to -23) within the 1B promoter of DMT1 increased the expression of DMT1 in undifferentiated P19 embryonic carcinoma cells (Paradkar and Roth, 2006a,b). This indicated NF-κB might be involved in the regulation of DMT1 expression in MPP$^+$-treated cells, and Rg1 might regulate the expression of DMT1-IRE through inhibiting NF-κB activation. Therefore, we detected the protein levels of NF-κB in different groups. As we expected, MPP$^+$ could activate NF-κB translocation from cytoplasm to nucleus. And this could be inhibited by Rg1, indicating Rg1 plays a role in NF-κB regulation and subsequent gene regulation, and this may be the mechanism of neuroprotective activity of Rg1 on DMT1 up-regulation. This is further supported by the application of BAY 11-7082, an inhibitor of IκBα phosphorylation and degradation, which can inhibit the activation of NF-κB. Pretreated with BAY 11-7082 could abolish the MPP$^+$-induced up-regulation of DMT1-IRE.

We have demonstrated that Rg1 could inhibit the ROS production in MPP$^+$-treated MES23.5 cells. Then whether the antioxidant effect of Rg1 contributes to its inhibition of NF-κB in MPP$^+$ treated MES23.5 cells? Evidence proved that oxidative stress-induced ROS generation has been implicated in NF-κB activation (Pyo et al., 2008). Therefore, MPP$^+$-induced oxidative stress may contribute to increased NF-κB nuclear translocation and binding activity response to MPP$^+$, and Rg1 might have the regulatory effect on NF-κB and DMT1-IRE by its antioxidant. To confirm this hypothesis, NAC, a free radical scavenger, was used in this study. As we expected, results showed NAC pretreatment led to an efficient inhibitory effect on MPP$^+$-induced translocation of NF-κB and the

up-regulation of DMT1-IRE. This suggests that oxidative stress is involved in up-regulation of DMT1-IRE response to MPP$^+$ through activation of NF-κB, and Rg1 had the ability to regulate the expression of DMT1-IRE by inhibiting ROS-NF-κB pathway.

MPP$^+$ increased DMT1-IRE expression and enhanced ferrous iron influx in MES23.5 cells. The increased intracellular ferrous iron will interact with hydrogen peroxide to form hydroxyl radicals, which causes the mitochondria dysfunction. We observed increased ROS production and decreased mitochondria membrane potential in MPP$^+$ treated cells followed by iron incubation. Rg1 showed inhibitory effect on this increased iron influx and iron-induced cell damage, indicating that Rg1 could exert its neuroprotective effect through regulating the cellular iron levels and inhibiting iron-induced cell damage. This implicated the new pharmacological effect of Rg1 on iron accumulation.

In conclusion, we reported that the neuroprotective effects of Rg1 against MPP$^+$ toxicity was through preventing the improper up-regulation of DMT1-IRE, decreasing the cellular iron influx and iron-induced cell damage. And this effect may contribute to its inhibitory effect on the production of ROS and the activation of NF-κB. Further studies should be carried out to evaluate whether ginsenoside-Rg1 could benefit as a future preventive and therapeutic drug of PD.

References

Aruoma, O.I., Halliwell, B., Hoey, B.M., Butler, J., 1989. The antioxidant action of N-acetylcysteine: its reaction with hydrogen peroxide, hydroxyl radical, superoxide, and hypochlorous acid. Free Radic. Biol. Med. 6, 593–597.

Burdo, J.R., Menzies, S.L., Simpson, I.A., Garrick, L.M., Garrick, M.D., Dolan, K.G., Haile, D.J., Beard, J.L., Connor, J.R., 2001. Distribution of divalent metal transporter 1 and metal transport protein 1 in the normal and Belgrade rat. J. Neurosci. Res. 66, 1198–1207.

Cassarino, D.S., Parks, J.K., Parker Jr., W.D., Bennett Jr., J.P., 1999. The parkinsonian neurotoxin MPP$^+$ opens the mitochondrial permeability transition pore and releases cytochrome c in isolated mitochondria via an oxidative mechanism. Biochim. Biophys. Acta 1453, 49–62.

Chen, X.C., Zhou, Y.C., Chen, Y., Zhu, Y.G., Fang, F., Chen, L.M., 2005. Ginsenoside Rg1 reduces MPTP-induced substantia nigra neuron loss by suppressing oxidative stress. Acta Pharmacol. Sin 26, 56–62.

Chen, X.C., Zhu, Y.G., Zhu, L.A., Huang, C., Chen, Y., Chen, L.M., Fang, F., Zhou, Y.C., Zhao, C.H., 2003. Ginsenoside Rg1 attenuates dopamine-induced apoptosis in PC12 cells by suppressing oxidative stress. Eur. J. Pharmacol. 473, 1–7.

Cheng, Y., Shen, L.H., Zhang, J.T., 2005. Anti-amnestic and anti-aging effects of ginsenoside Rg1 and Rb1 and its mechanism of action. Acta Pharmacol. Sin 26, 143–149.

Chwa, M., Atilano, S.R., Reddy, V., Jordan, N., Kim, D.W., Kenney, M.C., 2006. Increased stress-induced generation of reactive oxygen species and apoptosis in human keratoconus fibroblasts. Invest. Ophthalmol. Vis. Sci. 47, 1902–1910.

Crawford Jr., G.D., Le, W.D., Smith, R.G., Xie, W.J., Stefani, E., Appel, S.H., 1992. A novel N18TG2 x mesencephalon cell hybrid expresses properties that suggest a dopaminergic cell line of substantia nigra origin. J. Neurosci. 12, 3392–3398.

Desai, V.G., Feuers, R.J., Hart, R.W., Ali, S.F., 1996. MPP(+)-induced neurotoxicity in mouse is age-dependent: evidenced by the selective inhibition of complexes of electron transport. Brain Res. 715, 1–8.

Faucheux, B.A., Hirsch, E.C., Villares, J., Selimi, F., Mouatt-Prigent, A., Javoy-Agid, F., Hauw, J.J., Agid, Y., 1993. Distribution of 125I-ferrotransferrin binding sites in the mesencephalon of control subjects and patients with Parkinson's disease. J. Neurochem. 60, 2338–2341.

Gunshin, H., Mackenzie, B., Berger, U.V., Gunshin, Y., Romero, M.F., Boron, W.F., Nussberger, S., Gollan, J.L., Hediger, M.A., 1997. Cloning and characterization of a mammalian proton-coupled metal-ion transporter. Nature 388, 482–488.

He, Y., Lee, T., Leong, S.K., 1999. Time-course and localization of transferrin receptor expression in the substantia nigra of 6-hydroxydopamine-induced parkinsonian rats. Neuroscience 91, 579–585.

Huang, E., Ong, W.Y., Go, M.L., Connor, J.R., 2006. Upregulation of iron regulatory proteins and divalent metal transporter-1 isoforms in the rat hippocampus after kainate induced neuronal injury. Exp. Brain Res. 170, 376–386.

Hubert, N., Hentze, M.W., 2002. Previously uncharacterized isoforms of divalent metal transporter (DMT)-1: implications for regulation and cellular function. Proc. Natl. Acad. Sci. U S A 99, 12345–12350.

Jiang, H., Qian, Z.M., Xie, J.X., 2003. Increased DMT1 expression and iron content in MPTP-treated C57BL/6 mice. Sheng Li Xue Bao 55, 571–576.

Jiang, H., Song, N., Wang, J., Ren, L.Y., Xie, J.X., 2007. Peripheral iron dextran induced degeneration of dopaminergic neurons in rat substantia nigra. Neurochem. Int. 51, 32–36.

Lee, P.L., Gelbart, T., West, C., Halloran, C., Beutler, E., 1998. The human Nramp2 gene: characterization of the gene structure, alternative splicing, promoter region and polymorphisms. Blood Cells Mol. Dis. 24, 199–215.

Lenardo, M.J., Baltimore, D., 1989. NF-kappa B: a pleiotropic mediator of inducible and tissue-specific gene control. Cell 58, 227–229.

Leung, K.W., Yung, K.K., Mak, N.K., Chan, Y.S., Fan, T.P., Wong, R.N., 2007. Neuroprotective effects of ginsenoside-Rg1 in primary nigral neurons against rotenone toxicity. Neuropharmacology 52, 827–835.

Lim, J.H., Wen, T.C., Matsuda, S., Tanaka, J., Maeda, N., Peng, H., Aburaya, J., Ishihara, K., Sakanaka, M., 1997. Protection of ischemic hippocampal neurons by ginsenoside Rb1, a main ingredient of ginseng root. Neurosci. Res. 28, 191–200.

Lopez, M.V., Cuadrado, M.P., Ruiz-Poveda, O.M., Del Fresno, A.M., Accame, M.E., 2007. Neuroprotective effect of individual ginsenosides on astrocytes primary culture. Biochim. Biophys. Acta 1770, 1308–1316.

Oertel, W.H., Ellgring, H., 1995. Parkinson's disease–medical education and psychosocial aspects. Patient Educ. Couns. 26, 71–79.

Pahl, H.L., Baeuerle, P.A., 1997. The ER-overload response: activation of NF-kappa B. Trends Biochem. Sci. 22, 63–67.

Paradkar, P.N., Roth, J.A., 2006a. Nitric oxide transcriptionally down-regulates specific isoforms of divalent metal transporter (DMT1) via NF-kappaB. J. Neurochem. 96, 1768–1777.

Paradkar, P.N., Roth, J.A., 2006b. Post-translational and transcriptional regulation of DMT1 during P19 embryonic carcinoma cell differentiation by retinoic acid. Biochem. J. 394, 173–183.

Picard, V., Govoni, G., Jabado, N., Gros, P., 2000. Nramp 2 (DCT1/DMT1) expressed at the plasma membrane transports iron and other divalent cations into a calcein-accessible cytoplasmic pool. J. Biol. Chem. 275, 35738–35745.

Pierce, J.W., Schoenleber, R., Jesmok, G., Best, J., Moore, S.A., Collins, T., Gerritsen, M.E., 1997. Novel inhibitors of cytokine-induced IkappaBalpha phosphorylation and endothelial cell adhesion molecule expression show anti-inflammatory effects in vivo. J. Biol. Chem. 272, 21096–21103.

Pyo, C.W., Yang, Y.L., Yoo, N.K., Choi, S.Y., 2008. Reactive oxygen species activate HIV long terminal repeat via post-translational control of NF-kappaB. Biochem. Biophys. Res. Commun. 376, 180–185.

Salazar, J., Mena, N., Hunot, S., Prigent, A., Alvarez-Fischer, D., Arredondo, M., Duyckaerts, C., Sazdovitch, V., Zhao, L., Garrick, L.M., Nunez, M.T., Garrick, M.D., Raisman-Vozari, R., Hirsch, E.C., 2008. Divalent metal transporter 1 (DMT1) contributes to neurodegeneration in animal models of Parkinson's disease. Proc. Natl. Acad. Sci. U S A 105, 18578–18583.

Wakabayashi, C., Murakami, K., Hasegawa, H., Murata, J., Saiki, I., 1998. An intestinal bacterial metabolite of ginseng protopanaxadiol saponins has the ability to induce apoptosis in tumor cells. Biochem. Biophys. Res. Commun. 246, 725–730.

Wang, J., Jiang, H., Xie, J.X., 2007. Ferroportin1 and hephaestin are involved in the nigral iron accumulation of 6-OHDA-lesioned rats. Eur. J. Neurosci. 25, 2766–2772.

Wang, J., Xu, H.M., Yang, H.D., Du, X.X., Jiang, H., Xie, J.X., 2009. Rg1 reduces nigral iron levels of MPTP-treated C57BL6 mice by regulating certain iron transport proteins. Neurochem. Int. 54, 43–48.

Wetli, H.A., Buckett, P.D., Wessling-Resnick, M., 2006. Small-molecule screening identifies the selanazal drug ebselen as a potent inhibitor of DMT1-mediated iron uptake. Chem. Biol. 13, 965–972.

Woods, M., Wood, E.G., Mitchell, J.A., Warner, T.D., 2000. Signal transduction pathways involved in cytokine stimulation of endothelin-1 release from human vascular smooth muscle cells. J. Cardiovasc. Pharmacol. 36, S407–S409.

Yang, J., Su, Y., Richmond, A., 2007. Antioxidants tiron and N-acetyl-L-cysteine differentially mediate apoptosis in melanoma cells via a reactive oxygen species-independent NF-kappaB pathway. Free Radic. Biol. Med. 42, 1369–1380.

Yao, K., Wu, W., Wang, K., Ni, S., Ye, P., Yu, Y., Ye, J., Sun, L., 2008. Electromagnetic noise inhibits radiofrequency radiation-induced DNA damage and reactive oxygen species increase in human lens epithelial cells. Mol. Vis. 14, 964–969.

Youdim, M.B., Stephenson, G., Ben Shachar, D., 2004. Ironing iron out in Parkinson's disease and other neurodegenerative diseases with iron chelators: a lesson from 6-hydroxydopamine and iron chelators, desferal and VK-28. Ann. N. Y Acad. Sci. 1012, 306–325.

Zecca, L., Casella, L., Albertini, A., Bellei, C., Zucca, F.A., Engelen, M., Zadlo, A., Szewczyk, G., Zareba, M., Sarna, T., 2008. Neuromelanin can protect against iron-mediated oxidative damage in system modeling iron overload of brain aging and Parkinson's disease. J. Neurochem. 106, 1866–1875.

Zhang, S., Wang, J., Song, N., Xie, J., Jiang, H., 2009. Up-regulation of divalent metal transporter 1 is involved in 1-methyl-4-phenylpyridinium (MPP(+))-induced apoptosis in MES23.5 cells. Neurobiol. Aging 30, 1466–1476.

Zhong, G., Jiang, Y., 1997. Calcium channel blockage and anti-free-radical actions of ginsenosides. Chin. Med. J. (Engl) 110, 28–29.